Stability and Performance Analysis of HIPERLAN

G. Anastasi, L. Lenzini, and E. Mingozzi

Dept. of Information Engineering, University of Pisa, Via Diotisalvi 2, I- 56126 Pisa (Italy)
{anastasi, lenzini, mingozzi}@iet.unipi.it

Abstract. *This paper thoroughly analyses the HIPERLAN MAC protocol, which is a standard for Wireless Local Area Networks (WLANs) defined by the European Telecommunications Standards Institute (ETSI). Since the HIPERLAN MAC protocol belongs to the class of Carrier Sensing Multiple Access with Collision Avoidance (CSMA/CA), in the first part of the paper we analyze the HIPERLAN stability problem. In the second part we present an in depth performance analysis, by simulation, of the HIPERLAN MAC protocol. The analysis is performed by considering data traffic patterns (hereafter advanced data traffic) which have a very similar shape to traffic generated by WWW applications. Furthermore, in the analysis we consider Poissonian data traffic too. Our conclusion is that the HIPERLAN MAC protocol performs satisfactorily, although performance measures with advanced traffic are worse than the corresponding performance measures with Poissonian traffic. Furthermore, we broadened our analysis to include the influence of the packet lifetime and channel access priority mechanism on the performance measures provided by HIPERLAN.*

1 Introduction

HIPERLAN is a standard for a Wireless Local Area Network (WLAN) defined by the European Telecommunications Standards Institute (ETSI). HIPERLAN supports the ad-hoc topology only along with the multihop routing capability to forward packets from a source to a destination which cannot communicate directly [4].

The HIPERLAN MAC protocol explicitly supports a quality of service (QoS) for packet delivery which is provided via two mechanisms: the user priority of a packet (high or low) and the packet lifetime (default value, 500 ms). The residual lifetime of a packet together with its user priority[1] are used to determine its Channel Access Mechanism (CAM) priority which can fall into one of five priority levels. Since multihop routing is supported within the standard the lifetime of a packet and the residual lifetime are transmitted along with the packet. Packets that cannot be delivered within the allocated lifetime are discarded.

In [14] a HIPERLAN performance analysis is reported in order to check the suitability of HIPERLAN to become a candidate for the upcoming Wireless ATM (WATM) MAC protocol. Furthermore, a comparison between HIPERLAN and IEEE 802.11 (the other very well known proposal for wireless LAN) can be found in [16].

The aim of this paper is to further advance previous analyses in the following directions:

- stability analysis according to the stability definition given in [9]. This requires the computation of the HIPERLAN MAC protocol capacity which is defined as the maximum utilization of the radio channel over all possible offered loads [1];
- evaluation of the QoS provided by HIPERLAN to advanced data applications. In fact, since we expect relevant data applications serviced by WLANs to very much resemble today's WWW applications, in our performance analysis we use data traffic models which are very similar to those recently proposed in the literature for these type of applications (i.e., WWW applications) [3], [2].

Since we evaluate the HIPERLAN performances with one class of data traffic we only take into consideration the low user priority. Although data integrity is a key requirement for data transmission, we assume an error free radio channel despite the fact that we are dealing with a very unreliable environment. This is because in the present paper we are focusing on multiple access aspects of the HIPERLAN MAC protocol as measured by the average access delay experienced by packets transmitted over data connections. Furthermore, we do not take into consideration the hidden node and capture problems.

The paper is organized as follows. Section 2 describes the HIPERLAN MAC protocol. Section 3 reports the stability analysis while Section 4 is devoted to the performance analysis. Section 5 concludes the paper.

2 The Channel Access Mechanism

The HIPERLAN channel access mechanism is based on channel sensing and a contention resolution scheme called *Elimination Yield - Non-preemptive Priority Multiple Access* (EY-NPMA). In the following, *EY-NPMA scheme* and *MAC protocol* expressions are used interchangeably. According to the HIPERLAN channel access mechanism, channel status is sensed by each node having a data frame to be transmitted. If the channel is sensed idle for at least 1700 bit-periods, then the channel is considered free, and the node is allowed to immediately start transmission of the data frame. Each data frame transmission must be explicitly acknowledged by an ACK transmission from the destination node. On the other hand, whenever a frame transmission is desired and the channel is considered not free, then, according to HIPERLAN terminology, a channel access with synchronization takes place.

Synchronization is performed to the end of the current transmission interval, and, at that point in time, a channel access cycle begins according to the EY-NPMA scheme. The channel access cycle consists of three phases: the prioritization phase, the contention phase and the transmission phase. In Figure 1 an example of a channel access cycle with synchronisation is represented.

The aim of the prioritization phase is to allow only nodes with the highest channel access priority frame, among the contending ones, to participate in the next phase. In HIPERLAN

[1] The initial values of both parameters are assigned by the user.

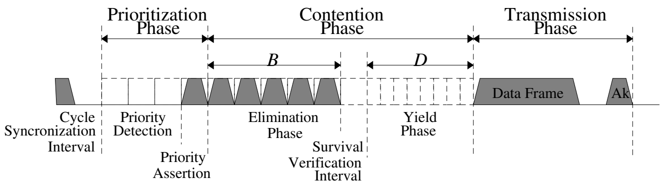

Fig. 1. Channel Access Cycle with Synchronisation.

a priority level h is assigned to each frame. Priority levels are numbered from 0 to $H-1$, with 0 denoting the highest priority level. The prioritization phase consists of at most H prioritization slots, each 256 bit-periods long. Each node that has a frame with priority level h senses the channel for the first h prioritization slots (Priority Detection). If the channel is idle during this interval, then the node transmits a burst in the $h+1$-th slot (Priority Assertion) and it is admitted to the contention phase, otherwise it stops contending and waits for the next channel access cycle.

The contention phase starts immediately after the transmission of the prioritization burst, and it further consists of two phases: the elimination phase and the yield phase.

The elimination phase consists of at most n elimination slots, each 256 bit-periods long, followed by a 256 bit-periods long elimination survival verification slot. Starting from the first elimination slot, each node transmits a burst for a number B, $0 \le B \le n$, of subsequent elimination slots, according to the following truncated geometric probability distribution function:

$$\Pr\{B=b\} = \begin{cases} (1-q)q^b & 0 \le b < n \\ q^n & b = n \end{cases} \qquad (1)$$

After the end of the burst transmission, each node senses the channel for the duration of the elimination survival verification slot. If the channel is sensed idle, the node is admitted to the yield phase, otherwise it drops itself from contention and waits for the next channel access cycle.

The yield phase starts immediately after the end of the elimination survival verification interval and consists of at most m yield slots, each 64 bit-periods long. Each node listens to the channel for a number D, $0 \le D \le m$, of yield slots before (if allowed) beginning transmission. D is an r.v. with truncated geometric distribution as follows:

$$\Pr\{D=d\} = \begin{cases} (1-p)p^d & 0 \le d < m \\ p^m & d = m \end{cases} \qquad (2)$$

If the channel is sensed idle during the yield listening interval, the node is allowed to begin the transmission phase, otherwise the node loses contention and waits for the next channel access cycle. The operation parameter settings, according to HIPERLAN, are reported in Table 1.

Elimination and yield phases are complementary to each other. As it will be proved in the next section, elimination phase drastically reduces to a few the number N of nodes taking part to the channel access cycle, and this result is remarkably achieved almost independently of N. The yield phase, which has good performance with a small number of contending nodes, further reduces the number of nodes allowed to transmit possibly to one. Furthermore, it is noteworthy that with EY-NPMA at least one node will always be allowed to transmit.

Real time traffic transmission is supported in HIPERLAN by dinamically varying the CAM priority depending upon the user priority and the packet residual lifetime as reported in Table 2.

Table 1. Operation Parameter Settings.

Parameter	Value
Channel Bit Rate (Mbit/sec)	23.5
Channel Access Mechanism Priority Levels (H)	5
Maximum number of subseq. Elimination bursts (n)	12
Probability of bursting in an Elimination slot (q)	0.5
Maximum number of subseq. Yield listenings (m)	14
Probability of listening in a Yield slot (p)	0.9

Table 2. Computation of the CAM priority.

	High User Priority	Low User Priority
NMRL < 10 msec	0	1
10 msec ≤ NMRL < 20 msec	1	2
20 msec ≤ NMRL < 40 msec	2	3
40 msec ≤ NMRL < 80 msec	3	4
80 msec ≤ NMRL	4	4

The user priority is an attribute which is assigned to each packet according to the type of traffic carried by and it determines the maximum CAM priority value the packet may eventually reach. The residual packet lifetime is the time interval within which the transmission of the packet must occur before the packet has to be discarded. Since multihop routing is supported within the standard, the residual packet lifetime (NMRL = Normalized MPDU Residual Lifetime) is normalized to the number of hops the packet has to traverse to reach the final destination.

3 Stability Analysis

In this section we derive analytical results regarding throughput and delay related to EY-NPMA. Main results, as a function of the operation parameters of the protocol, are reported in Table 3.

A. MAC Protocol Capacity

In the following analysis, we assume that N nodes that have the same priority level start a channel access cycle with synchronisation. Let B_i represent the length (in elimination slot periods) of the elimination burst transmitted by the i-th node, $1 \le i \le N$. The probability distribution function of B_i is given by (1). Let S_i be an r.v. defined as follows:

$$S_i = \begin{cases} 1 & B_i = \max_{1 \le j \le N} B_j \\ 0 & \text{otherwise} \end{cases} \qquad (3)$$

S_i is one if and only if node i is admitted to the yield phase. Since B_k, $1 \le k \le N$, are independent and identically distributed random variables, conditioning upon the value of B_i, it follows that:

$$\Pr\{S_i = 1\} = \sum_{j=0}^{n} \Pr\{B=j\} \Pr\{B \le j\}^{N-1} \qquad (4)$$

Let S represent the number of nodes that survive the elimination phase. The probability distribution function of S is derived conditioning upon the length of the burst transmitted by surviving nodes:

$$\Pr\{S=s\} = \binom{N}{s} \sum_{j=0}^{n} \Pr\{B=j\}^s \Pr\{B<j\}^{N-s} \qquad (5)$$

Since, by definition:

$$S = \sum_{i=1}^{N} S_i$$

Table 3. Main Analytical Results.

$\Pr\{S_i = 1\}$	$\sum_{j=0}^{n-1}(1-q)q^j\left(1-q^{j+1}\right)^{N-1}+q^n$
$\Pr\{S = s\}$	$\binom{N}{s}\left(\sum_{j=0}^{n-1}\left((1-q)q^j\right)^s\left(1-q^j\right)^{N-s}+\left(q^n\right)^s\left(1-q^n\right)^{N-s}\right)$
$\Pr\{T_i = 1 \mid S = s\}$	$\begin{cases}\sum_{j=0}^{m-1}(1-p)p^j\left(p^{j+1}\right)^{s-1} & s>1\\ 1 & s=1\end{cases}$
$\Pr\{T = 1\}$	$N\sum_{j=0}^{m-1}(1-p)p^j\left(\sum_{i=0}^{n-1}(1-q)q^i\left(1-q^i\left(1-(1-q)p^{j+1}\right)\right)^{N-1}+q^n\left(1-q^n\left(1-p^{j+1}\right)\right)^{N-1}\right)+$ $+Np^m\left(\sum_{i=0}^{n-1}(1-q)q^i\left(1-q^i\right)^{N-1}+q^n\left(1-q^n\right)^{N-1}\right)$
$E[L_E]$	$1+n-\sum_{l=1}^{n}\left(1-q^l\right)^N$
$E[L_Y]$	$\sum_{l=0}^{m-1}\left(\sum_{j=0}^{n-1}\left(\left(1-q^j\left(1-(1-q)p^{l+1}\right)\right)^N-\left(1-q^j\right)^N\right)+\left(1-q^n\left(1-p^{l+1}\right)\right)^N-\left(1-q^n\right)^N\right)$

it immediately follows that:

$$E[S] = NE[S_i] = N\Pr\{S_i = 1\} \tag{6}$$

Let D_i represent the interval (in yield slot periods) of channel listening by node i before (if allowed) beginning data transmission. D_i's, $1 \le i \le N$, are independent and identically distributed random variables according to (2). Let T_i be an r.v. defined as follows:

$$T_i = \begin{cases}1 & D_i < D_k, 1 \le k \le N, k \ne i\\ 0 & \text{otherwise}\end{cases} \tag{7}$$

T_i is one if and only if node i successfully transmits a data frame. The probability of such an event, conditioned upon the number S of nodes that survived the elimination phase, is:

$$\Pr\{T_i = 1 \mid S = s\} = \sum_{j=0}^{m}\Pr\{D = j\}\Pr\{D > j\}^{s-1} \tag{8}$$

Let T be an r.v. which is one if and only if a successful transmission occurs at the end of the contention phase. Since the events $\{T_i = 1\}$, $1 \le i \le N$, mutually exclude each other, it follows that:

$$\Pr\{T = 1 \mid S = s\} = s\Pr\{T_i = 1 \mid S = s\} \tag{9}$$

and, finally, by combining (5) and (9):

$$\Pr\{T = 1\} = \sum_{s=1}^{N}\Pr\{T = 1 \mid S = s\}\Pr\{S = s\} \tag{10}$$

which represents the probability of a successful transmission when N nodes, with the same priority level, access the channel.

B. *Stability*

The aim of a contention resolution scheme is to avoid the channel saturation phenomenon in which a rise in channel input rate reduces the channel throughput which in turn further increases the channel input rate. The system may periodically recover from channel saturation, but eventually return to it (and then exhibit a bistable behaviour) or it will be unable to recover and thus breaks down. This phenomenon was first highlighted for slotted-Aloha by Kleinrock and Lam in [9], where a stability definition was introduced to characterize the dynamic behaviour of the protocol. More recently, the same undesirable behaviour has been highlighted in other random access protocols, such as R-Aloha and PRMA [15], [12], [13]. In this subsection, we will follow Kleinrock's line of reasoning to demonstrate that HIPERLAN does not exhibit a bistable behaviour.

Let us consider a system of M nodes, in which each node transmits packets of the maximum allowed size (19080 bits according to HIPERLAN standard). With no loss of generality, we may assume that each packet has the same priority level $h = 1$ and each packet source is blocked until the previous generated packet has been successfully transmitted. Let N represent the number of backlogged nodes, i.e., the number of nodes out of M that have a packet to transmit. If $N > 1$ then N nodes access the channel according to EY-NPMA, and equation (10) gives us the probability of a successful transmission in one access cycle. By taking into consideration the overhead introduced by the MAC layer[2] and the contention protocol (which has a variable size due to variable elimination-yield phases duration), we can derive the following equation for the average net throughput (as a percentage of the available bandwidth) carried out over the channel:

$$T_{OUT} = \frac{19080 \cdot \Pr\{T = 1\}}{25970 + E[L]}$$

where $\Pr\{T = 1\}$ is the probability of successful transmission given by (10) and $E[L]$ is the average bit overhead introduced by the elimination and yield phases. An analytical expression for this quantity is derived below. Let L_E (L_Y) represent the length

[2] We assume that user bits are carried by a DT-HMPDU type 0, see [4] for details.

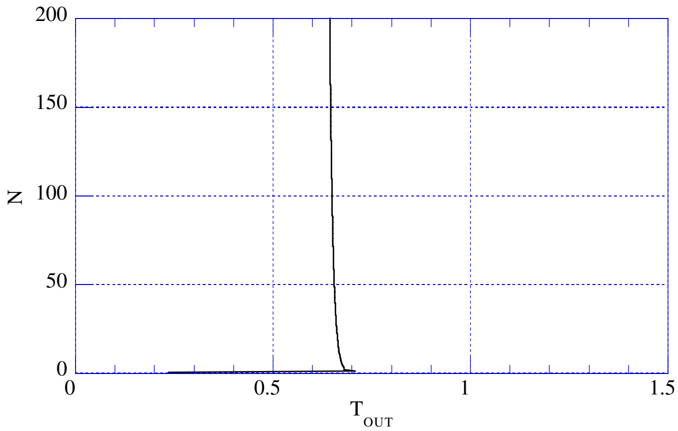

Fig. 2. Equilibrium contour in (T_{OUT}, N) plane.

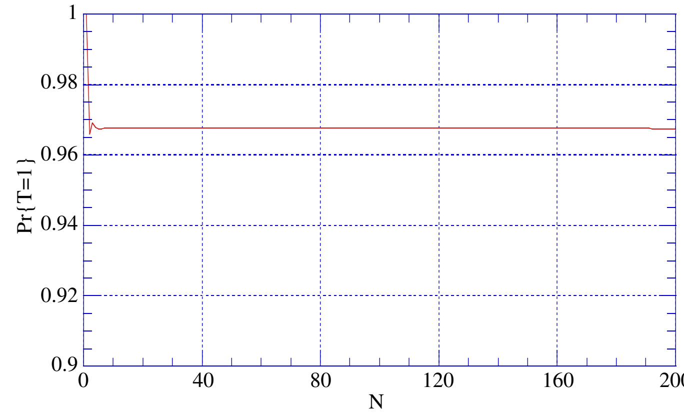

Fig. 3. Probability of successful transmission.

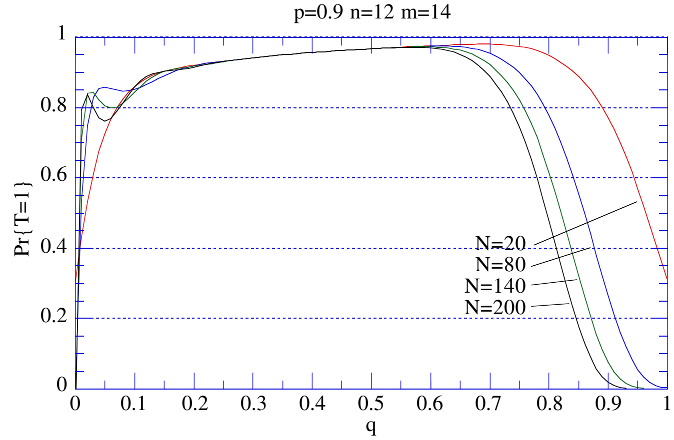

Fig. 4. Probability of successful transmission as a function of q.

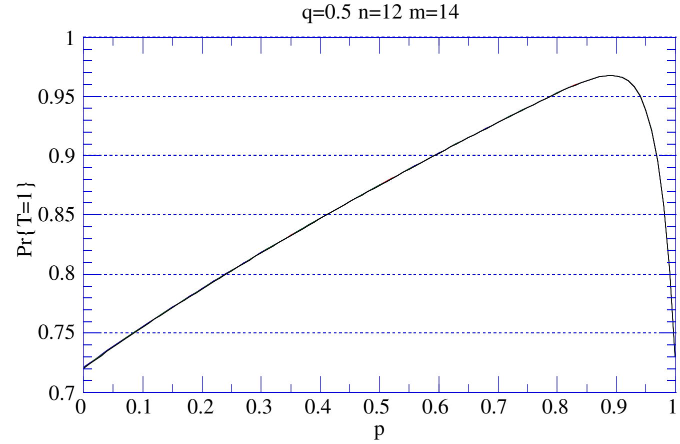

Fig. 5. Probability of successful transmission as a function of p.

of the elimination (yield) phase in elimination (yield) slots. Then:

$$L_E = 1 + \max_{1 \le i \le N} B_i$$

$$L_{Y|S} = \min_S D_i$$

where S is the total number of nodes that survive the elimination phase. The average values of L_E and L_Y may be computed by applying some basic results of the probability theory and are reported in Table 3. The average bit overhead is:

$$E[L] = 256 \cdot E[L_E] + 64 \cdot E[L_Y]$$

An equilibrium contour in the (T_{OUT}, N) plane is depicted in Figure 2, according to the operation parameter settings of Table 1.

The channel operating point (i.e., the statistical equilibrium point operation of the system) is obtained by intersecting the equilibrium contour with an input load line given by the following equation:

$$T_{IN} = \sigma(M - N)$$

where σ is the average input rate at each node (normalized to the available bandwidth).

Figure 2 highlights that any particular load line will always intersect the equilibrium contour in just one point. The reason is that EY-NPMA throughput gracefully degrades from its maximum for all values of N, thus not exhibiting that sudden decrease which is responsible for the saturation phenomenon. Hence, according to Kleinrock's definition, the channel operation under EY-NPMA is always stable.

C. *Sensitivity analysis*

In the previous subsection an expression for the probability of successful transmission in a channel access cycle with synchronisation was derived.

Figure 3 shows the probability of successful transmission as a function of the number N of contending nodes. Note that this probability is very close to one and decreases very slowly with the number of contending nodes, so that the variation is not valuable in the range of reasonable values of N. This property of EY-NPMA is due to a correct setting of the operation parameters, as is clear from Figures 4 and 5.

In fact, Figure 4 shows the probability of successful transmission as a function of q and with the other parameter values set according to HIPERLAN standard, for different values of N. Clearly, there is a range of q values that results in a superposition of the curves representing the probability of successful transmission. Within this range the standard value of $q = 0.5$ was chosen.

The same probability values from equation (10) are reported in Figure 5 as a function of p. Although the probability values are represented for different values of N (as in Figure 4), in this case there is a superposition of curves for the entire range of p values, so that a single curve in fact seems to appear in Figure 5. The value of $p = 0.9$ was chosen in order to optimize the performance of the channel access contention resolution mechanism.

4 Performance Analysis

The main difficulty for the performance analysis of the HIPERLAN MAC protocol via analytical models is the high degree of complexity and interdependence of the various processes that are involved in the MAC protocol operation. Therefore, to evaluate the performances of the protocol we designed an *ad hoc* simulator and implemented it in C++ language.

This section is structured into four subsections. In the first we introduce the traffic model used during the simulative analysis and in the second subsection the measures of interest are defined. In the third subsection the system and traffic parameters are defined and in the last subsection simulation results are presented and discussed.

4.1 Traffic Characterization

In our simulation experiments we considered non real-time data type of traffic. Generally, when modelling data traffic, packet arrival processes are often assumed to be Poissonian. However, this model does not capture any correlation between consecutive packet arrivals which is, on the other hand, exhibited by experimental data [6], [11]. To recover from this problem MMPP (Markov Modulated Poisson Process) data traffic models have been proposed [6], [7].

One of the characteristics of MMPP processes is that the sojourn time in each state of the underlying Markov chain is exponentially distributed. However, recent teletraffic studies have shown that experimental data related to WWW applications can be satisfactorily modeled by ON/OFF processes where the ON and OFF time-length distributions are heavily tailed (e.g., Weibull, Pareto). By aggregating a large number of such ON/OFF sources the resulting traffic process exhibits self-similar properties [17].

It might be useful to recall that the Weibull probability distribution function of a random variable X is

$$P\{X \le x\} = 1 - e^{-(x/\beta)^{\alpha}}, \quad x \ge 0$$

where $\alpha > 0$ and $\beta > 0$ are real, and are called shape and scale parameters, respectively. Note that when $\alpha = 1$ the Weibull distribution is reduced to an exponential distribution, and then the ON/OFF process becomes an MMPP, while when α decreases (with $\alpha < 1$) the tail of the distribution tends to become more and more heavily tailed, i.e., the burstiness of the packet arrivals tends to increase. For the purpose of our simulation analysis we used a fixed packet size.

4.2 Performance Measures

This section introduces the performance measures (or indices) used to characterize the quality of service (QoS) provided by the HIPERLAN MAC protocol. The indices defined in our analysis to specify the QoS are a widely accepted, minimum set of performance measures used to characterize the performance of any computer network. Before introducing the performance measures we observe that packets are queued in a node *local queue* as soon as they arrive. Therefore, except when the node is empty, a packet will experience some delay in the local queue before contending for the channel according to the HIPERLAN MAC protocol. With this in mind, the performance measures we use in our analysis are defined below:

- *average queueing delay*: average time elapsed from the time a packet joins the local queue *up until* it reaches the head of the local queue itself: i.e., it starts contending for the channel;

Table 4. Traffic Parameter Values.

Traffic Parameter	Parameter Value
Node Offered Load	100 Kbit/sec
Average ON duration	3.3 sec
Average OFF duration	22.8 sec

- *average MAC delay*: the average delay experienced by a packet from the time it reaches the head of the local queue up until the beginning of its successful transmission. The rationale behind this choice is that the average MAC delay measures the delay caused by the MAC protocol, and thus measures the interference between a user on one node and the users on the other nodes. Furthermore, the average MAC delay does not include the average queueing delay experienced by a packet while queued in the local node queue, i.e., it does not take into account the interference between users on the same node;
- *average access delay*: sum of the average MAC delay and the average queueing delay in the local queue;
- *aggregate throughput*: average number of bits successfully transmitted by all nodes per time unit;
- *packet discard probability*: fraction of discarded packets due to deadline expiration.

4.3 Operation Parameter Settings

The system parameters for our simulation environment are those recommended by the standard [4], [5] and are reported in Table 1. Traffic related parameters are reported in Table 4. Specifically, the data node offered load value of 100 Kbit/sec was chosen to cover a broad range of data services; on the other hand although the ON and OFF durations are different from the values in [3], they nevertheless allow reasonable execution times for simulation experiments without altering the stochastic nature of the arrival process. Packet size was chosen to be constant and equal to 19,080 bits (i.e., the maximum length defined in the standard [4]).

4.4 Simulation Results for Data Traffic

In this section we report and comment on, in terms of MAC protocol mechanisms, the simulation results we obtained with the arrival processes and operation parameter settings previously specified. In all the experiments discussed in this section all the nodes have infinite buffers and are assumed to contribute with the same offered load.

A. Influence of the arrival processes

In the curves reported below we compare Poisson and ON/OFF processes, where ON/OFF period lengths are Weibull distributed with $\alpha = 1$ (MMPP) and $\alpha < 1$.

Figure 6 shows the aggregate throughput achieved by HIPERLAN vs the number of data nodes. This figure highlights that the throughput curves which refer to the various arrival data processes tend to diverge when the number of nodes goes beyond 130. All curves tend towards horizontal asymptotes, which may differ from one curve to the other, when the number of data nodes goes beyond 130.

The higher throughput for Poisson arrivals can be justified by looking at Figure 7 which reports the discard probability vs the number of data nodes for the same arrival processes considered in Figure 6. This figure highlights that the discard probability for Poisson arrivals is lower than for the ON/OFF arrivals. Furthermore for the latter class of arrival processes the

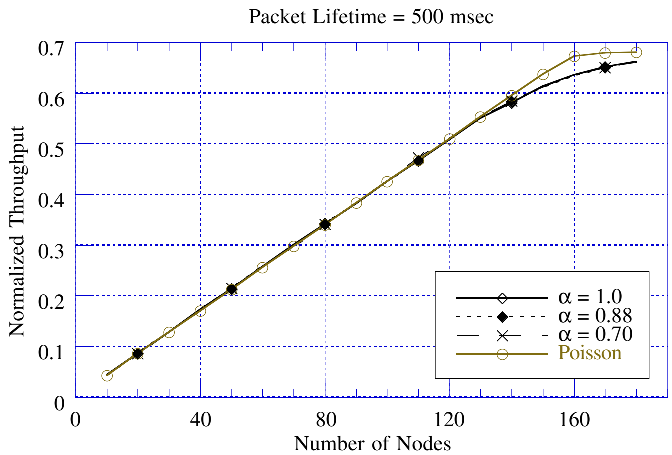

Fig. 6. Aggregate throughput vs the number of data sources for different arrival processes.

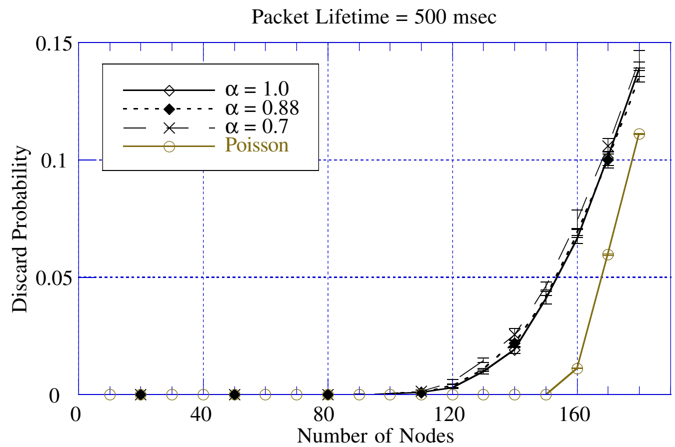

Fig. 7. Discard probability vs the number of data sources for different arrival processes.

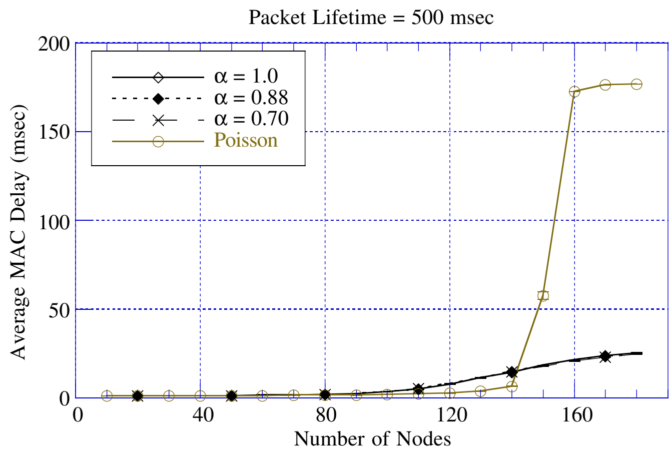

Fig. 8. Average MAC delay for several values of α and Poisson.

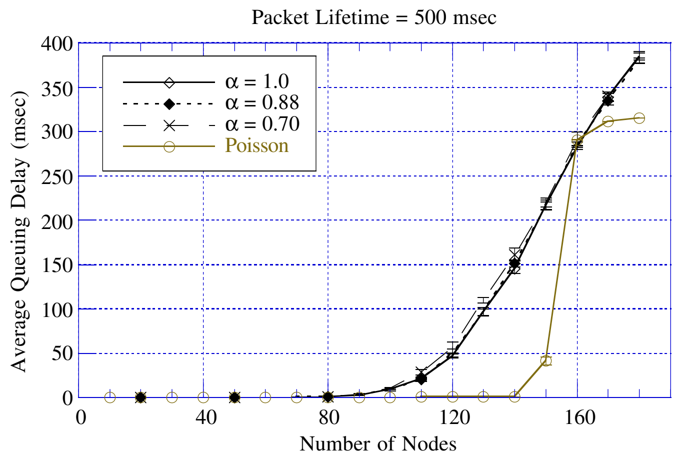

Fig. 9. Average queueing delay for several values of α and Poisson.

discard probability increases slightly when the α value decreases (i.e., the burstiness increases). This will be explained later in the section. However, from the throughput standpoint the variation in burstiness in the ON/OFF arrival processes does not produce any meaningful difference. The asymptotic behaviour of the throughput curves are in accordance with the analytic results shown in Figure 2.

Figure 8 reports the average MAC delay experienced by any packet in any data node when the arrival process is Poissonian and ON/OFF. In the latter case we considered several α values. This figure shows that the average MAC delays of the various ON/OFF arrival processes almost overlap. On the other hand, the average MAC delay curve related to the Poissonian arrival process deviates considerably from the ON/OFF curves.

The different shape of the MAC delay curves for Poissonian arrivals and ON/OFF arrivals can be explained in terms of burstiness. In fact, when the arrival process is Poisson, packets arrive uniformly distributed over any time interval while for ON/OFF packets are generated only by the nodes which are in the ON periods (and which are very likely to be a subset of the overall number of nodes). Hence, when the arrival process is Poisson, the aggregate offered load is uniformly distributed among all the nodes while for ON/OFF process the aggregate offered load is concentrated on the node subsets which are in the ON period. Hence, the number of contending nodes with Poisson traffic is greater than the corresponding number with ON/OFF traffic. This explains the fact that the average MAC delay for Poissonian arrivals is greater than the average MAC delay for ON/OFF arrivals, at least when the number of nodes is greater than approximately 130 (see Figure 8).

When the number of nodes is below 130 the opposite behavior holds, i.e., the average MAC delay for Poissonian traffic is lower than the average MAC delay for ON/OFF traffic. This can be justified by the fact that the aggregate offered load is well below the channel capacity and hence the number of nodes which have frames to transmit is low. This implies that the "active" nodes have a high probability to perform immediate transmissions (i.e., bypassing the three phases). This probability is lower with ON/OFF than with Poisson, since packets with the former arrival process tend to arrive back to back.

Figure 9 shows the average queueing delay versus the number of data nodes for the arrival processes already considered in the analysis of the average MAC delay. The shape of the curves reported in Figure 9 is similar to the shape of the curves related to the average MAC delay reported in Figure 8. As expected, due to the burstiness, the average queueing delay with ON/OFF processes is greater than with a Poisson process.

The average access delay curves reported in Figure 10 can be easily obtained by summing up the contributions of the average MAC and queueing delay components reported in Figures 8 and 9. From this figure it follows that with a number of nodes up to 140 the average MAC delay is almost zero with Poissonian

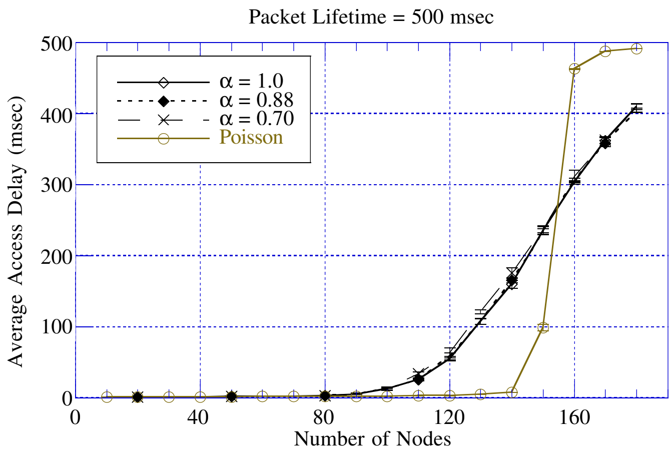

Fig. 10. Average access delay versus the number of nodes for several values of α and Poisson.

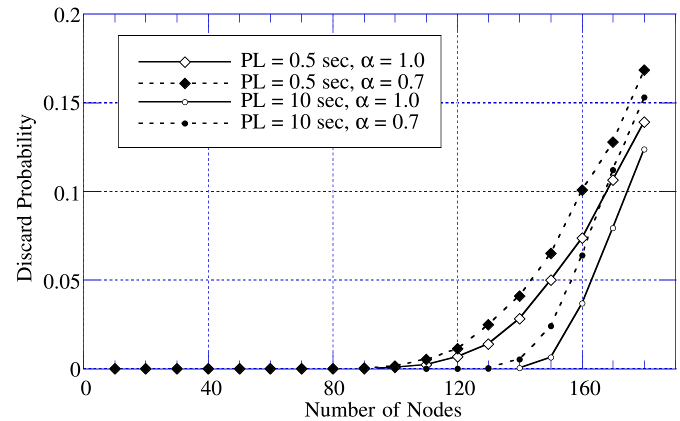

Fig. 11. Discard probability versus the number of nodes when the packet lifetime is 0.5 sec and 10 sec.

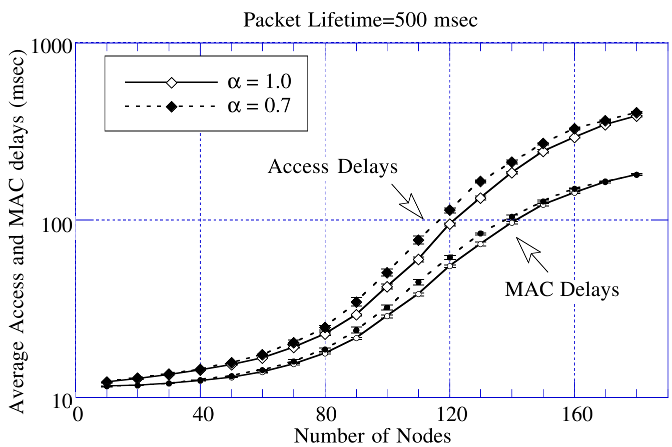

Fig. 12: Average access and MAC delay versus the number of nodes when the packet lifetime is 500 msec.

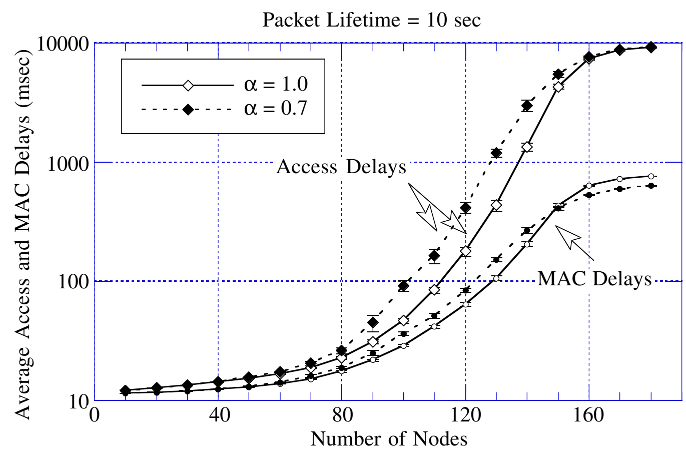

Fig. 13. Average access and MAC delay versus the number of nodes when the packet lifetime is 10 secs.

traffic and very low (approximately 150 msec) with ON/OFF traffic.

B. *Influence of the packet lifetime*

Figures 8, 9 and 10 highlight that, for ON/OFF processes the MAC and queueing delays do not depend on the values of α (i.e., burstiness). At first sight this may appear surprising. To investigate this we made simulation experiments with several packet lifetimes. To reduce the simulation time when the packet lifetime is much higher than 500 msec, we reduced the medium channel capacity to 2.3 Mbps. Consequently the offered load of each node was reduced by a factor of 10 (i.e., from 100 Kbps to 10 Kbps). Figure 11 reports a comparison between the discard probability (vs the number of nodes) for packet lifetimes of 0.5 sec and 10 sec (for a network capacity of 2.3 Mbps). Figure 11 highlights that, at high offered loads:

- the packet discard probability drops considerably when passing from 0.5 sec to 10 sec;
- the effect of the values of α (i.e., burstiness) is observable also with a packet lifetime of 0.5 sec. This is due to the combined effect of the medium capacity and offered load reductions.

Figure 11 allow us to interpret the shapes of the curves in Figures 12 and 13 which report the average access and MAC delays for two values of both α and packet lifetimes vs the number of nodes. Specifically, the distance between the curves referring to the two α values is more noticeable at 10 sec than at 0.5 sec. This is due to the fact that the discard probability is lower at 10 sec than at 0.5 sec.

In conclusion, the behavior of Figures 8, 9 and 10 can now be explained by observing that by increasing the packet lifetime, the multiplexing capability increases with the consequence that the probability that a packet is discarded due to the expiration of the residual packet lifetime decreases. As a consequence, the sojourn time of a packet in the local queue increases and, hence, the burstiness of the arrival process has more and more influence.

C. *Influence of the CAM priorities*

The investigation of the influence of the CAM priorities on the performance measures is a formidable task since the number of scheduling disciplines that can be envisaged to access the channel is, in principle, very large. In the following we compare the performance measures obtained by the standard protocol with those obtained when the CAM priority is not a function of the packet residual lifetime. Hence packets at local queues are transmitted in a FIFO order.

Figure 14 highlights this difference in terms of discard probability for two values of α. As expected, the use of CAM priorities as recommended by the standard leads to a lower discard probability. The decrease in the packet discard probability when CAM priorities are used obviously influences the maximum

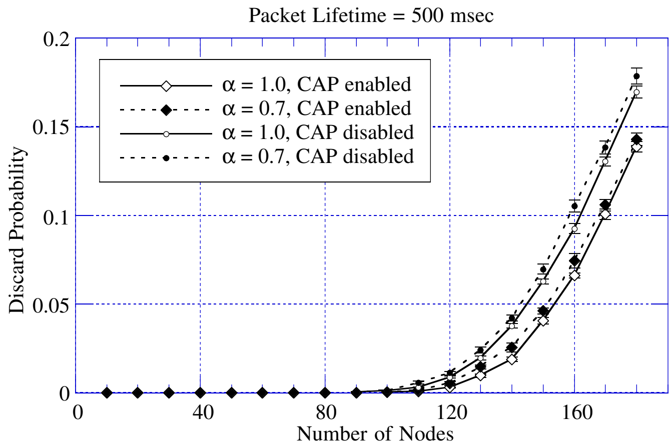

Fig. 14. Influence of CAM priorities on the discard probability for a 500 msec packet lifetime and two different α values.

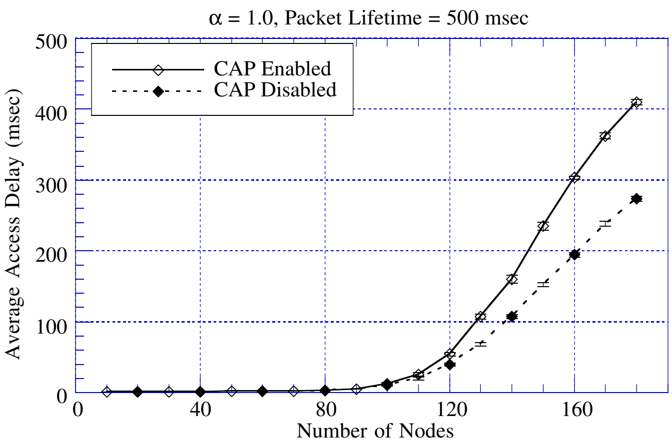

Fig. 16. Influence of CAM priorities on the average access delay.

aggregate throughput that the HIPERLAN MAC protocol can manage (see Figure 15) and the average access delay experienced by the various packets (see Figure 16). In fact, when the fraction of the discarded packets decreases, the aggregate throughput increases. At the same time, since the number of queued packets in each local queue increases, the access delay experienced by any packet increases. Note that the average access delay reported in Figure 16 relates to the fraction of packets which are successfully transmitted.

5 Conclusions

In the first part of this paper we performed a stability analysis of the HIPERLAN MAC protocol. The most important results obtained are that HIPERLAN is basically stable and that the probability values for the elimination (q) and for the yield (p) phases proposed by the standard are appropriate values. Furthermore, a closed formula for the HIPERLAN MAC capacity has been derived. From this formula we can draw the conclusion that the maximum aggregate throughput (i.e., MAC protocol capacity) which can be provided by HIPERLAN is approximately 65% of the channel bandwidth. In the second part of the paper we carried out a simulation analysis of the HIPERLAN MAC protocol. This analysis is based on "realistic" data traffic models which conform to the modern data network applications (e.g., WWW). From our analysis we can conclude that HIPERLAN performs satisfactorily and that the average

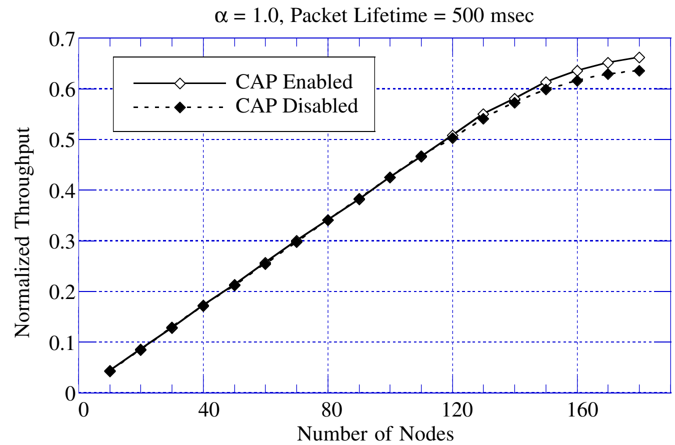

Fig. 15. Influence of CAM priorities on the normalized aggregate throughput.

access delay is strongly dependent on the data arrival process, packet lifetime and Channel Access Mechanism priorities.

References

[1] M. Conti, E. Gregori, L. Lenzini, "Metropolitan Area Networks", Springer-Verlag, 1996.

[2] M. E. Crovella, A. Bestavros, "Explaining World Wide Web Traffic Self-Similarity", Technical Report TR 95-015, Computer Science Dept., Boston University, August 29, 1995.

[3] S. Deng, "Empirical Model of WWW Document Arrivals at Access Link", *Proceedings of ICC '96*, June 23-27, 1996, Dallas, Texas, pp. 1797-1802.

[4] ETSI, "Hiperlan Functional Specification", ETSI Draft Standard, July 1995.

[5] ETSI TC-RES Report, "Hiperlan: Functional Specification", ETSI Technical Report, ETR 226, October 1995.

[6] R. Gusella, "Characterizing the Variability of Arrival Processes with Indexes of Dispersion", *IEEE Journal on Selected Areas in Communications*, vol. 9, no. 2, pp. 203-211, Feb. 1991.

[7] H. Heffes., D. M. Lucantoni, "A Markov Modulated Characterization of Packetized Voice and Data Traffic and Related Statistical Multiplexer Performance", *IEEE Journal on Selected Areas in Communications*, vol. 4, no. 6, Sept. 1986.

[8] P802.11/D2.1, Draft Standard IEEE 802.11, "Wireless LAN Medium Access Control (MAC) and Physical Layer (PHY) Specifications", December 4, 1995.

[9] S. L. Lam, L. Kleinrock, "Packet Switching in a Multiaccess Broadcast Channel: Performance Evaluation," *IEEE Transactions on Communications*, vol. 23, no. 4, pp. 410-423, Apr. 1975.

[10] R. O. LaMaire, A. Krishna, J. Panian, and P. Bhagwat, "Wireless LANs and Mobile Networking: Standards and Future Directions", IBM Corporation, December 22, 1995.

[11] W. E. Leland, M. S. Taqqu, W. Willinger, D. V. Wilson, "On the Self-Similar Nature of Ethernet Traffic", *IEEE/ACM Transactions on Networking*, vol. 2, no 1, pp. 1-15, Feb. 1994.

[12] S. Nanda, D. J. Goodman, and U. Timor, "Performance of PRMA: a Packet Voice Protocol for Cellular Systems," *IEEE Transactions on Vehicular Technology*, vol. 40, no.3, pp. 584-598, Aug. 1991.

[13] S. Nanda, "Stability Evaluation and Design of the PRMA Joint Voice Data System," *IEEE Transactions on Communications*, vol. 42, no. 5, pp. 2092-2104, May 1994.

[14] L. Nenonen and J. Mikkonen, "Wireless ATM MAC Performance Evaluation, Case Study: HIPERLAN vs. Modified MDR", Proceedings of ACM/IEEE Mobicom'96, Nov. 10-12, 1996, Rye, New York, pp. 165-175.

[15] S. Tasaka, "Stability and Performance of the R-ALOHA Packet Broadcast System," *IEEE Transactions on Computers*, vol. 32, no. 8, pp. 717-726, Aug. 1983.

[16] J. Weinmiller, M. Schlager, A. Festag, A. Wolisz, "Performance Study of Access Control in Wireless LANs - IEEE 802.11 DFWMAC and ETSI RES 10 HIPERLAN", *ACM/Baltzer Mobile Networks and Applications*, vol. 2, no. 1, pp. 55-67, 1997.

[17] W. Willinger, M. S. Taqqu, R. Sherman, D. V. Wilson, "Self-Similarity through High Variability Statistical Analysis of Ethernet LAN Traffic at the Source Level", *Proceedings of ACM SIGCOMM '95*, Aug. 28-Sept. 1, 1995, Cambridge, MA, pp. 100-113.